environmental microbiology reports

Environmental Microbiology Reports (2012) doi:10.1111/j.1758-2229.2012.00354.x

Unsuspected control of siderophore production by *N*-acetylglucosamine in streptomycetes

Matthias Craig,[1] Stéphany Lambert,[1] Samuel Jourdan,[1] Elodie Tenconi,[1] Séverine Colson,[1] Marta Maciejewska,[1] Marc Ongena,[2] Juan Francisco Martin,[3] Gilles van Wezel[4] and Sébastien Rigali[1]*

[1]*Centre for Protein Engineering, Université de Liège, Institut de chimie B6a, Liège B-4000, Belgium.*

[2]*Walloon Centre for Industrial Biology, Université de Liège/Gembloux Agro-Bio Tech, Gembloux B-5030, Belgium.*

[3]*Institute of Biotechnology of Léon, INBIOTEC, Parque Cientifico de Léon, Leon 24006, Spain.*

[4]*Microbial Development, Leiden Institute of Chemistry, Leiden University, PO Box 9502, 2300RA Leiden, the Netherlands.*

Summary

Iron is one of the most abundant elements on earth but is found in poorly soluble forms hardly accessible to microorganisms. To subsist, they have developed iron-chelating molecules called siderophores that capture this element in the environment and the resulting complexes are internalized by specific uptake systems. While biosynthesis of siderophores in many bacteria is regulated by iron availability and oxidative stress, we describe here a new type of regulation of siderophore production. We show that in *Streptomyces coelicolor*, their production is also controlled by *N*-acetylglucosamine (GlcNAc) via the direct transcriptional repression of the iron utilization repressor *dmdR1* by DasR, the GlcNAc utilization regulator. This regulatory nutrient–metal relationship is conserved among streptomycetes, which indicates that the link between GlcNAc utilization and iron uptake repression, however unsuspected, is the consequence of a successful evolutionary process. We describe here the molecular basis of a novel inhibitory mechanism of siderophore production that is independent of iron availability. We speculate that the regulatory connection between GlcNAc and siderophores might be associated with the competition for iron between streptomycetes and their fungal soil competitors, whose cell walls are built from the GlcNAc-containing polymer chitin. Alternatively, GlcNAc could emanate from streptomycetes' own peptidoglycan that goes through intense remodelling throughout their life cycle, thereby modulating the iron supply according to specific needs at different stages of their developmental programme.

Received 5 January, 2012; accepted 24 April, 2012. *For correspondence. E-mail srigali@ulg.ac.be; Tel. (+32) 4 366 98 30; Fax (+32) 4 366 33 64.

Introduction

Iron is an essential element, involved as it is in primary functions such as respiration, amino acid synthesis and DNA replication (Hantke, 2001). However, environmental ferric iron is poorly soluble and inassimilable by microorganisms (Greenwood and Earnshaw, 1997). To circumvent the low bioavailability of iron in the environment, bacteria and fungi biosynthesize and secrete high-affinity iron chelators, known as siderophores, to scavenge iron by forming soluble complexes that can be internalized and utilized for biochemical reactions (Kincade *et al.*, 1948; Crosa and Walsh, 2002; Wandersman and Delepelaire, 2004). Furthermore, siderophores are involved in many crucial biological processes. Indeed, microbial iron-chelators have been linked to fungi germination (Matzanke *et al.*, 1987), plant growth promotion (Compant *et al.*, 2005) and pathogen virulence as these molecules are required to scavenge iron from haem-containing intracellular proteins (e.g. haemoglobin) within the host (Ratledge and Dover, 2000; Miethke and Marahiel, 2007). In the soil-dwelling Gram-positive bacterial genus *Streptomyces*, siderophores have been shown to play a crucial role in sporulation and antibiotic or other secondary metabolite production as well as in the growth of some *Streptomyces* species unable to germinate under laboratory conditions (Yamanaka *et al.*, 2005).

Siderophore biosynthesis is tightly regulated in order to maintain adequate intracellular iron concentrations (Andrews *et al.*, 2003). Iron overload is hazardous to organisms, as Fe^{2+} ions trigger the Fenton reaction resulting in the production of harmful reactive oxygen species (ROS) (Galaris and Pantopoulos, 2008). Because ROS damage membranes, proteins and DNA, it is not surprising that siderophore production and oxidative stress responses are intimately coordinated (Andrews *et al.*, 2003; Cornelis *et al.*, 2011). Classically, siderophore

biosynthetic gene expression is controlled by transcriptional repressors that acquire or lose their DNA-binding capability depending on the intracellular concentration of ferrous iron (Braun, 1997; Lee and Helmann, 2007). However, the multiplicity and diversity of biological functions requiring the participation of siderophores suggests, on the contrary, vast heterogeneity in signals that control their production. Heat shock (Nielsen *et al*., 2010), high salinity (Hoffmann *et al*., 2002), anaerobic growth (Young and Postle, 1994) and hydrogen peroxide oxidative stress have been shown to affect iron-chelator biosynthesis (Touati, 2000). However, with the exception of the oxidative stress resistance mentioned above, the rationale for such regulatory connections has not been fully elucidated.

In our search for signalling molecules that might control the so-called secondary metabolite biosynthesis in streptomycetes, we previously discovered that the bacterial cell-wall aminosugar component *N*-acetylglucosamine (GlcNAc) is a potent agent in terms of the control of *Streptomyces* development (Rigali *et al*., 2006; 2008). The further discovery that the GlcNAc utilization regulator DasR (Deficient in aerial mycelium and spore formation Regulator) controls actinorhodin and prodiginine production in the model strain *Streptomyces coelicolor* by directly repressing expression of their pathway-specific regulators led to the identification of the first complete signalling cascade from nutrient transporters to antibiotic biosynthesis (Rigali *et al*., 2008). Recently, GlcNAc has been shown to induce antibiotic production in *Pseudomonas aeruginosa* as well, confirming the dual nutritive and signalling function of this molecule (Korgaonkar and Whiteley, 2011).

Herein, we provide evidence that biosynthesis of another category of microbial 'small molecules' produced by *Streptomyces* species, the tris-hydroxamate siderophores coelichelin (Lautru *et al*., 2005) and desferrioxamine (Barona-Gomez *et al*., 2004), is also controlled by the cell wall component GlcNAc. Our results have led us to the identification of a novel siderophore regulatory pathway that is, to our knowledge, the first described mechanism entirely independent of iron availability.

Results

N-*acetylglucosamine blocks siderophore production in streptomycetes*

In a previous work, we uncovered a nutrient-signalling pathway in streptomycetes in which GlcNAc is implicated in morphological differentiation and antibiotic production. This system is mediated via the GlcNAc-derived metabolic intermediate glucosamine-6P with the global regulator DasR (Rigali *et al*., 2006; 2008). We thus assessed the computational prediction of DasR-responsive elements (*dre*), as a potential strategy to identify natural products whose synthesis could be modulated by GlcNAc. Interestingly, scanning the genome of *S. coelicolor* highlighted a putative *dre* upstream of the gene *dmdR1* (divalent metal-dependent regulator) coding for the iron uptake repressor that regulates biosynthesis of the siderophores coelichelin and desferrioxamine (Flores and Martin, 2004; Tunca *et al*., 2007). To investigate the predicted control of iron homeostasis by GlcNAc, *S. coelicolor* M512 was grown on the iron limited (3 μM; Kieser *et al*., 2000) R2YE solid medium supplemented or not with GlcNAc (Fig. 1A) and the iron-chelating molecules were extracted from the spent agar. We selected the *S. coelicolor* M512 mutant as our model strain due to its inability to produce the pigmented metabolites actinorhodin and prodiginine that would otherwise interfere with the colorimetric siderophore production chrome azurol S (CAS) assay (Schwyn and Neilands, 1987). In line with previous observations for the parental strain M145 (Rigali *et al*., 2006), when *S. coelicolor* M512 was streaked on R2YE plates supplemented with GlcNAc, it displayed developmental arrest in the vegetative growth phase (Fig. 1A). CAS agar diffusion assays revealed high siderophore production in the extracts from R2YE cultures, while detection of siderophores was hardly visible in the extracts collected from the same cultures but supplemented with GlcNAc (Fig. 1B). High-performance liquid chromatography (HPLC) profiles revealed that the production of all structural forms of siderophores identified in *S. coelicolor* (Barona-Gomez *et al*., 2006), i.e. ferricoelichelin (CCLIN), ferrioxamine B (FOB) and ferrioxamine E (FOE), was drastically reduced upon addition of GlcNAc (Fig. 1C). LC-MS analysis of M512 extracts confirmed the identity of the three tri-hydroxamate siderophores (Fig. S1). Subsequent relative quantification revealed that coelichelin and desferrioxamine B and E production was 165-, 25- and 5-fold greater, respectively, in the R2YE culture extracts without exogenous GlcNAc supply (Fig. 1D).

To further confirm the link between GlcNAc and iron utilization, six different *Streptomyces* species (Fig. 2A–F) were tested for their capacity to produce siderophores with GlcNAc as the main carbon and nitrogen source. CAS assays and HPLC analyses revealed a significant reduction of iron-chelating molecules in *Streptomyces acrimycini*, *S. antibioticus*, *S. cacaoi*, *S. lividans* and *S. venezuelae*, while a slight reduction of only one type of siderophore (probably desferrioxamine B) was observed in *Streptomyces avermitilis* (Fig. 2F). This suggests that the GlcNAc-blocking effect on siderophore production is not limited to the model strain *S. coelicolor* but rather widespread among streptomycetes.

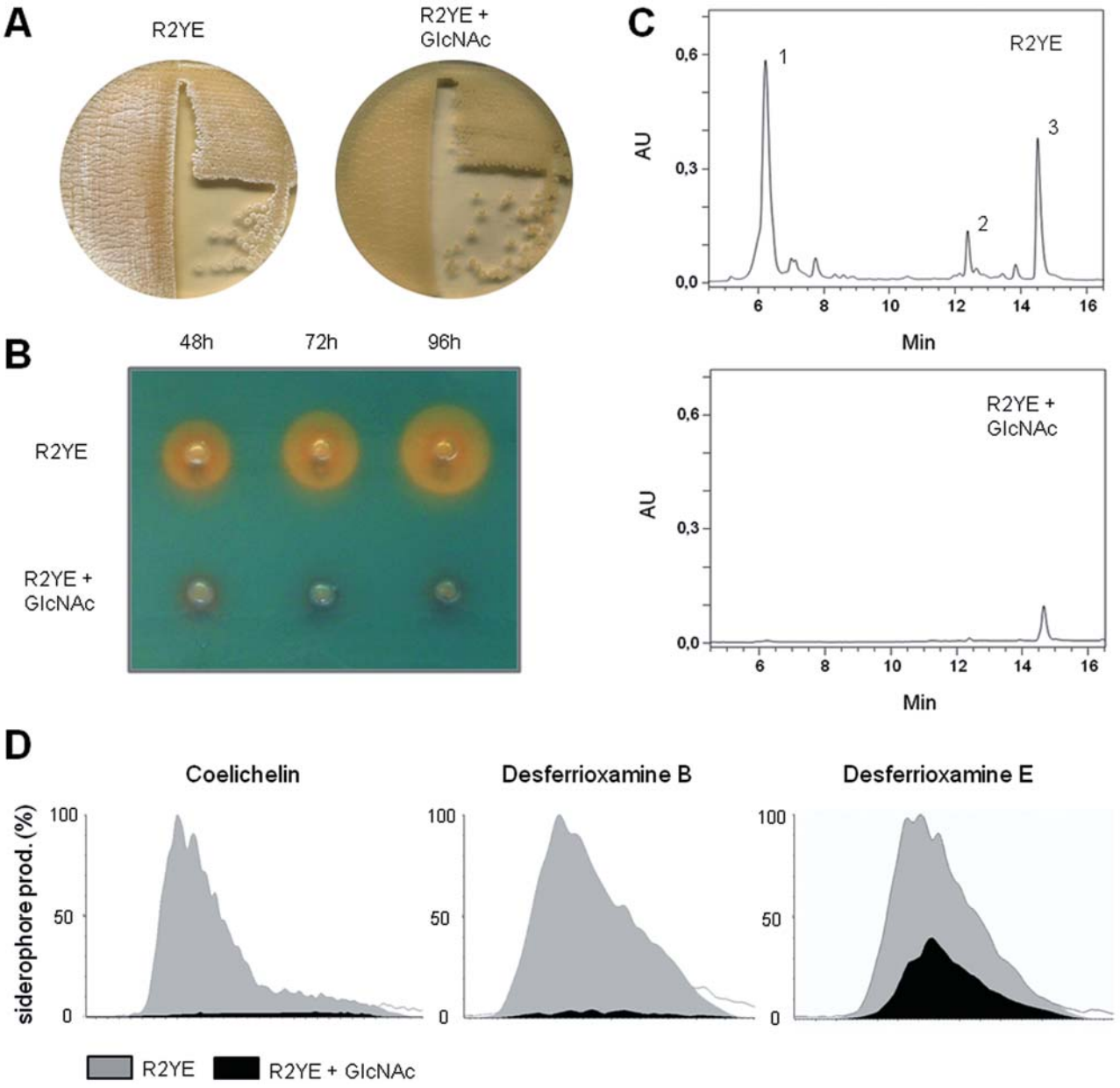

Fig. 1. *N*-acetylglucosamine blocks siderophore production in *S. coelicolor*.
A. Phenotype of the *S. coelicolor* pigmented-null mutant M512 grown for 96 h on R2YE agar plates with or without additional GlcNAc (50 mM). Note the lack of aerial hyphae (white filaments) in the presence of GlcNAc.
B. CAS siderophore production assay of *S. coelicolor* M512 extracellular extracts obtained from mycelia grown for 48, 72 or 96 h on R2YE plates with (bottom) or without GlcNAc (top).
C. HPLC analyses of the spent culture media (extracellular fractions) obtained from *S. coelicolor* M512 cultures grown for 96 h on R2YE agar plates with or without GlcNAc. Peaks annotated 1, 2 and 3 correspond to coelichelin (CCLIN), ferrioxamine B (FOB) and ferrioxamine E (FOE) respectively.
D. Comparison of the peak areas (black, R2YE+GlcNAc; grey, R2YE) corresponding to the siderophores CCLIN, DFOB and DFOE detected by LC-MS analysis of the extracellular fractions.

A signalling pathway from GlcNAc transport to siderophore biosynthesis

As stated earlier, the specific molecular basis of the GlcNAc-related pathway leading to siderophore biosynthesis inhibition is suggested by the computational prediction of *dre* in *S. coelicolor*. We identified the tgcGGTCTgGACCAGT *dre*-like sequence (*dre*^{dmdR1}) that shares 12 of the 16 bp of the *in silico*-deduced consensus *dre* (ACTGGTCTAGACCAGT) at position −184 relative to

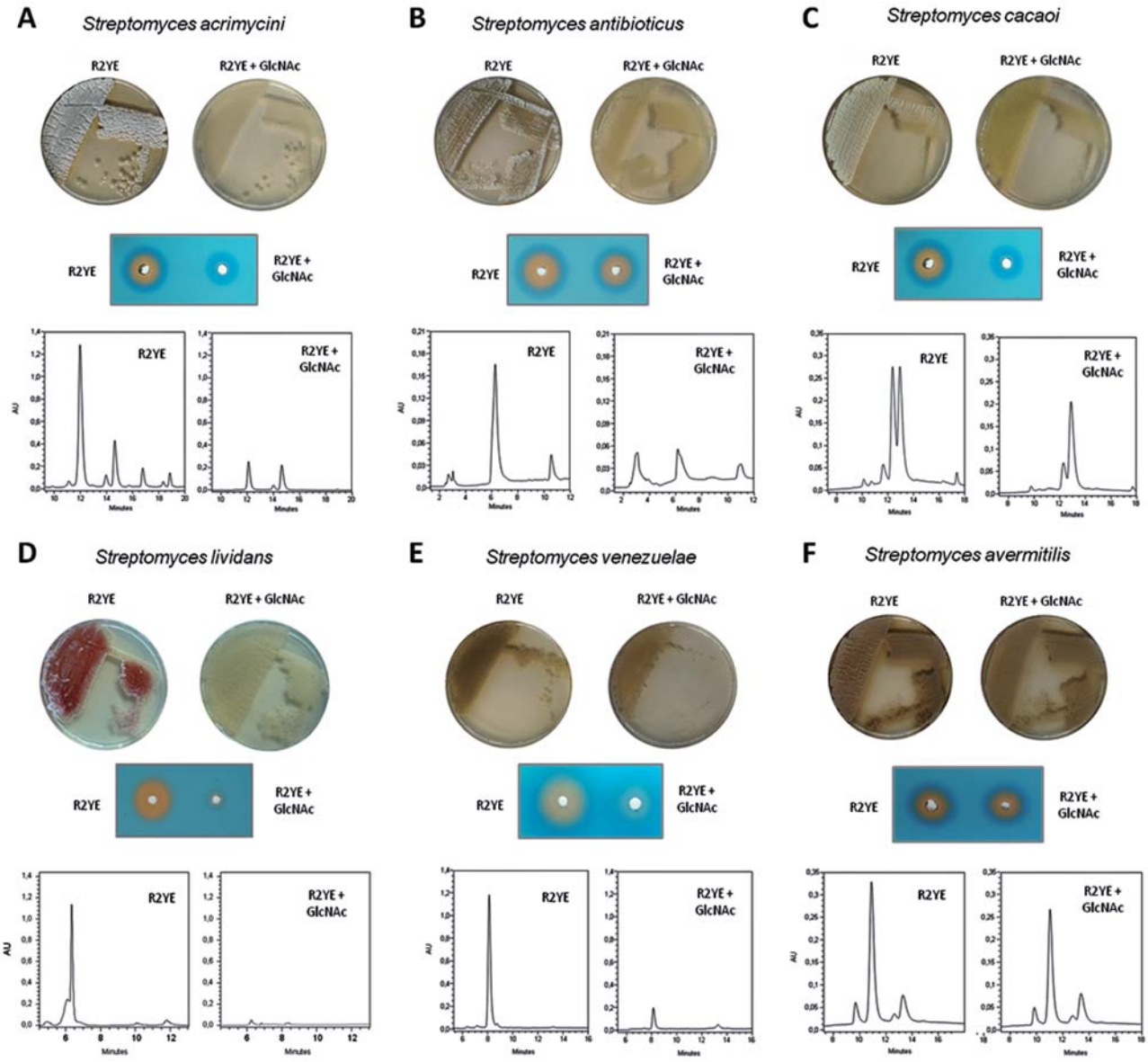

Fig. 2. The repression of siderophore synthesis by GlcNAc is conserved among *Streptomyces* species. Siderophores were extracted from cultures of six streptomycete species grown for 96 h on R2YE with or without 50 mM GlcNAc. The repressing effect of GlcNAc was assessed through CAS assay and HPLC analysis. Siderophore production was totally or greatly inhibited for all strain tested except for *S. avermitilis*. Interestingly, the addition of GlcNAc resulted in the blockage of the morphological development at the vegetative mycelium stage and/or in the inhibition of pigmented antibiotic synthesis for the six strains tested although the effect was less visible for *S. avermitilis* and *S. venezuelae*.

the translation start of *dmdR1* (see Table S1 for the complete DasR regulon predicted in *S. coelicolor*). Electrophoretic mobility gel shift assays (EMSA) with purified His_6-tagged DasR and a 40 bp Cy5-labelled probe centred on dre^{dmdR1} showed positive and specific protein/DNA interaction (Fig. 3A). Indeed, a 20-fold excess of unlabelled dre^{dmdR1} probe was necessary for full dissociation of the DasR/*dre* complex (Fig. 3A). The effect of GlcNAc or *dasR* deletion on *dmdR1* expression was further assessed by semi-quantitative reverse transcription polymerase chain reaction (RT-PCR) on RNA isolated from the *S. coelicolor* parental strain M145 and its *dasR* knockout mutant from solid cultures in MM mannitol or in R2YE with or without addition of 50 mM GlcNAc. Results presented in Fig. 3B and C demonstrate that *dmdR1* expression is induced by GlcNAc and repressed by DasR as observed for the GlcNAc-dependent and DasR-repressed control gene *nagE2* coding for the GlcNAc-specific permease.

These results strongly suggest a direct signalling pathway starting with GlcNAc transport and leading to the inhibition of siderophore biosynthesis in streptomycetes

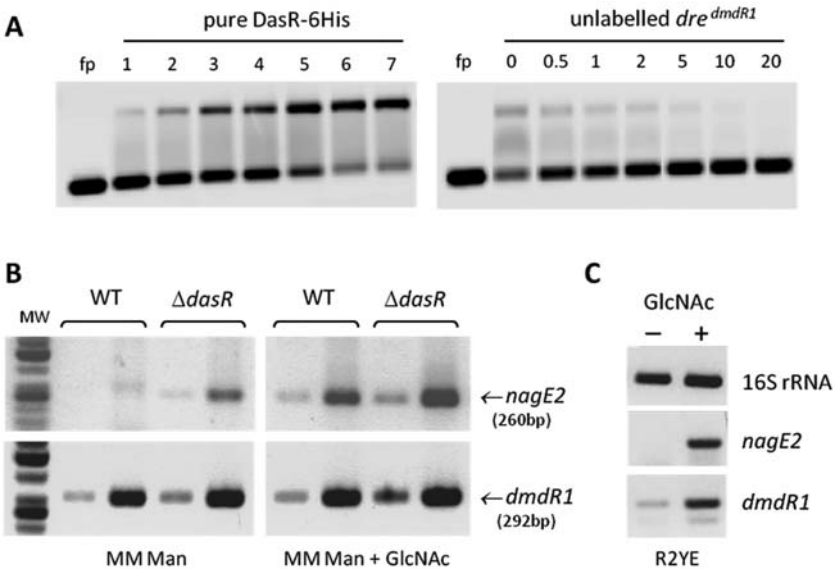

Fig. 3. *dmdR1* expression is induced by GlcNAc and repressed by DasR.
A. DasR binds *dre*^{dmdR1}. In the left panel, EMSA performed with 15 pmol of Cy5-labelled *dre*^{dmdR1} probe (fb, free probe) and increasing concentrations of pure DasR-6His (50, 75, 100, 125, 150, 175 and 200 pmol). In the right panel, EMSA with 15 pmol of the Cy5-labelled *dre*^{dmdR1} and 200 pmol of DasR-6His with increasing concentrations (from 0- to 20-fold excess) of the *dre*^{dmdR1} unlabelled probe. Note that a 20-fold excess of unlabelled probe is required to completely prevent DasR-His$_6$ interaction with the Cy5-labelled *dre*^{dmdR1} probe.
B and C. *dmdR1* expression is induced by *N*-acetylglucosamine and repressed by DasR. (B) Semi-quantitative RT-PCR on RNAs extracted from *S. coelicolor* M145 (WT, wild type) and its *dasR* knockout (Δ*dasR*) mutant grown on MM mannitol agar plates with or without addition of 50 mM GlcNAc. For semi-quantitative analyses, samples were taken at four-cycle intervals between cycles 28 and 36 so as to compare non-saturated PCR product formation (samples collected after 28 and 32 cycles are presented here). The deletion of *dasR* resulted in a 2.2-fold increased expression of *dmdR1*. Note that GlcNAc is still able to induce expression of *dmdR1* in the Δ*dasR* background. (C) RNA samples were collected from *S. coelicolor* M145 grown for 31 h at 28°C on R2YE agar plates with or without GlcNAc (50 mM). The 16S rRNA and *nagE2* genes were used as controls for GlcNAc-independent and GlcNAc-dependent genes respectively. Note that the addition of GlcNAc results in a sixfold higher expression of *dmdR1*, while expression of *nagE2* was dependent on GlcNAc (no *nagE2* transcripts were identified in the absence of GlcNAc). Expression of 16S rRNA was similar under both conditions (1.25 times more expression in the presence of GlcNAc).

(Fig. 4A). GlcNAc is transported and phosphorylated into *N*-acetylglucosamine-6-phosphate (GlcNAc-6P) by the GlcNAc-specific phosphotransferase system (PTS^{GlcNAc}), and GlcNAc-6P is further deacetylated by NagA into glucosamine-6-phosphate (GlcN-6P) (Swiatek *et al.*, 2012). GlcN-6P is a key molecule in the GlcNAc signalling pathway as it acts as an allosteric effector of DasR by inhibiting its DNA-binding capability (Rigali *et al.*, 2006) resulting in the overexpression of *dmdR1*. The legitimacy of our model was tested by assessing the GlcNAc-dependent response of siderophore production in the *S. coelicolor* GlcNAc utilization-deficient Δ*nagE2* mutant (strain BAP5) impaired in GlcNAc transport and phosphorylation (Nothaft *et al.*, 2010). In line with our expectation, no significant changes in siderophore production were detected in extracts of the *nagE2* GlcNAc transport mutant grown with or without GlcNAc (Fig. 4B), demonstrating that the GlcNAc signal has to be internalized and phosphorylated for siderophore production to be affected.

In addition to the identified DasR-mediated inhibitory cascade, our results suggest the existence of an alternative and major GlcNAc-dependent mechanism for reducing siderophore production. Indeed, GlcNAc is still able to increase *dmdR1* expression in the *dasR* mutant (Fig. 3B) suggesting that, besides inhibiting DasR interaction with *dre*^{dmdR1}, GlcNAc also inhibits siderophore biosynthesis by targeting other unknown proteins involved in *dmdR1* transcription control. As shown in Fig. S2, *dasR* deletion in *S. lividans* (which is strongly related to *S. coelicolor*) causes a significant reduction in siderophore biosynthesis while exogenous supply of GlcNAc has an even more drastic effect. The combination of *dasR* deletion and an exogenous supply of GlcNAc fully inhibits siderophore production. Analysis of this alternative GlcNAc-mediated inhibitory pathway is currently under investigation.

Discussion

The *in silico* prediction of the DasR regulon in *S. coelicolor* unveiled an unsuspected but direct control of iron utilization by GlcNAc. Siderophore-mediated iron uptake has been previously shown to be controlled by many different environmental stimuli (see *Introduction*), although the regulatory networks implicated are still poorly understood. In this work, we present the molecular basis of a novel mechanism of siderophore biosynthesis

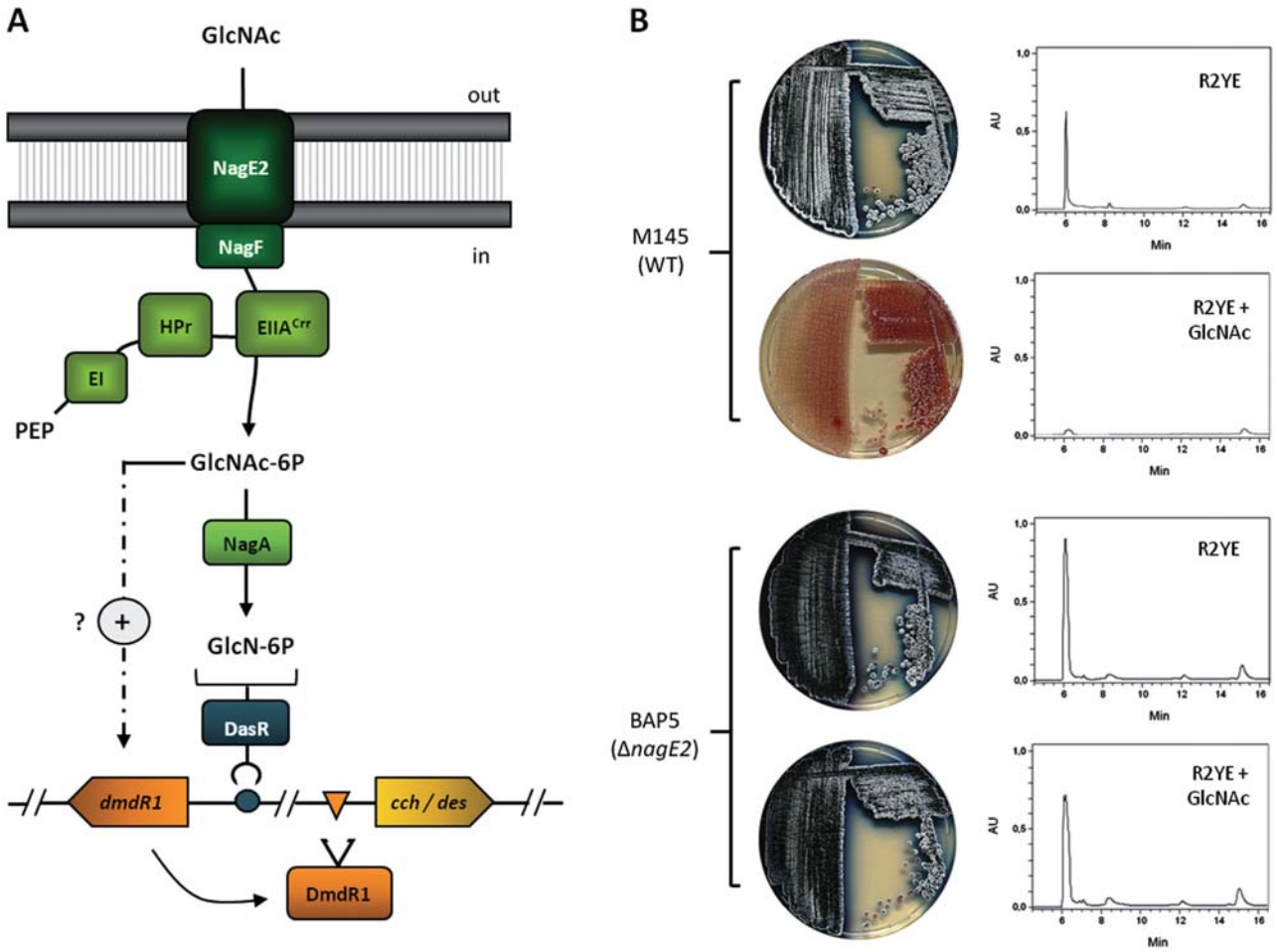

Fig. 4. Control of siderophore production by GlcNAc.
A. Deduced signalling cascade from GlcNAc transport to siderophore biosynthesis inhibition in streptomycetes. GlcNAc is transported and phosphorylated by the phosphotransferase system (PTS) comprised of the intracellular global components EI, HPr and EIIA, the GlcNAc-specific PTS component NagF, and permease NagE2. The intracellular *N*-acetylglucosamine-6-phosphate (GlcNAc-6P) is then deacetylated by NagA (GlcNAc-6P deacetylase) leading to glucosamine-6-phosphate (GlcN-6P), the allosteric effector of the GlcNAc utilization regulator DasR. Once complexed to GlcN-6P, DasR interaction with the *dre* upstream of *dmdR1* (blue circle) is weakened, which leads to increased *dmdR1* expression. The overexpression of *dmdR1* results in an increased transcriptional repression of siderophore biosynthetic clusters (*cch* and *des* for coelichelin and desferrioxamine biosynthesis respectively) due to DmdR1-Fe^{2+} binding to 'iron boxes' identified upstream of *cch* and *des* clusters (yellow triangle).
B. Deletion of GlcNAc permease *nagE2* cancels the GlcNAc-inhibiting effect on siderophore production. Left, phenotypes of *S. coelicolor* M145 (WT) and BAP5 (Δ*nagE2*) grown on R2YE plates with or without GlcNAc (50 mM). Note that GlcNAc is not able to block *S. coelicolor* development in a strain (BAP5) that cannot import GlcNAc. Right, HPLC profiles from extracts of *S. coelicolor* M145 and its Δ*nagE2* mutant showing the absence of the GlcNAc-blocking effect on siderophore production in strain BAP5.

inhibition that is the first, to our knowledge, to be entirely independent of environmental iron concentration. The inhibitory signalling cascade is in part mediated by the global regulator DasR linking GlcNAc utilization and development, although there is evidence supporting the existence of a yet unknown inhibitory circuit from GlcNAc uptake to the siderophore pathway-specific repressor DmdR1. We therefore anticipate the existence of a more complex regulatory network than in the model presented in Fig. 4.

Our work also exemplifies the importance of the phosphoenolpyruvate phosphotransferase system (PTS) in regulating essential biological processes in microorganisms. Very little is known on PTS-associated processes in actinobacteria. Next to participating to the transport of major nutrients such as GlcNAc or fructose (Nothaft *et al.*, 2003a; 2003b), there is no evidence that the PTS in streptomycetes and other actinobacteria is associated with the general mechanisms of carbon catabolite repression or inducer exclusion. Instead, previous works highlighted the crucial implication of general enzymes of the PTS and the associated transported molecule, in developmental processes such as sporulation or secondary metabolite production (Rigali *et al.*, 2006; 2008). Joseph

Deutscher and collaborators anticipated that future research would lead to the discovery of as-yet-unimagined biological processes controlled by the PTS (Deutscher *et al*., 2006). Our results highlighting the intimate regulatory connection between the PTS^{GlcNAc} and iron homeostasis perfectly illustrate that the roles of this phosphorelay system are not limited to the regulation of carbohydrate utilization.

Conservation of this inhibitory pathway in distantly related streptomycetes suggests that this unexpected regulatory event is the consequence of a successful evolutionary process. Interestingly, in *S. avermitilis* – the strain that responds to GlcNAc in a lesser manner in terms of siderophore biosynthesis (Fig. 2F) – we could not bioinformatically identify a reliable *dre* in the upstream region of the *dmdR1* orthologue. Hence, we anticipate that DasR does not interact (or less effectively) with the upstream region of the iron utilization repressor gene in this strain, which would explain the feeble repressing control of siderophore production exerted by GlcNAc. Furthermore, the examination of the transcriptome expression pattern of the *Bacillus subtilis* GlcNAc utilization regulator mutant Δ*nagR* (*nagR* being the orthologue of *dasR*) also revealed a similar negative control of GlcNAc on the iron depletion stimulon (Bertram *et al*., 2011). Although we have not yet identified the molecular basis of GlcNAc-based iron homeostasis control in *B. subtilis* the accumulation of evidence likely precludes a meaningless and fortuitous association.

The rationale for a direct control of iron homeostasis by GlcNAc – which is the most abundant carbon-nitrogen source on earth – is not self-evident. Different hypotheses for such an unusual regulatory relationship emerge depending on the source of GlcNAc in the streptomycetes environment. GlcNAc is a building block ubiquitously found in nature and GlcNAc-containing polymers such as chitin, chitosan and peptidoglycan, are major constituents of arthropod exoskeletons, filamentous fungi and bacterial cell walls (Schrempf, 2001). Filamentous fungi are important competitors of *Streptomyces* in the soil (Boer *et al*., 2005). They feature similar morphology and enzymatic capacity thus enabling them to colonize the same ecological niches. GlcNAc sensing by *Streptomyces* could indicate the presence of their fungal competitors in their immediate neighbourhood. As filamentous fungi have been reported to use *Streptomyces* desferioxamines (Boelaert *et al*., 1993), the GlcNAc-mediated siderophore inhibitory pathway may prevent fungi from accessing streptomycetes metabolites in the soil battle for iron.

If the cell wall of *Streptomyces* itself is the source of GlcNAc, the environmental context is entirely different. In this case, the presence of the amino sugar could indicate the occurrence of one of the several rounds of a programmed cell death process (Miguelez *et al*., 1999) that forms *a conditio sine qua non* to reach the later stages of the developmental programme (Manteca *et al*., 2005; 2006). Yamanaka and collaborators showed that siderophores, and thus iron, are crucial for sporulation and metabolite production in streptomycetes (Yamanaka *et al*., 2005). Our studies suggest that the blockage of the morphological development exerted by GlcNAc at the vegetative mycelium stage and the repression of siderophore biosynthesis might not be independent of each other. We postulate that the amino sugar GlcNAc emanating from the peptidoglycan could act as a signal molecule of bacterial cell wall integrity and therefore of the morphological stage of streptomycetes. In this manner, GlcNAc could dictate the entry or exit of the different morphological stages of the *Streptomyces* life cycle by modulating the exogenous supply of an element that has been proven to be essential in a microorganism's developmental programme. Elucidation of the physiological meaning of this regulatory network is currently under investigation.

Experimental procedures

Bacterial strains and culture conditions

Streptomyces coelicolor M145 and its pigmented [M512 (Floriano and Bibb, 1996), Δ*act*II-4 and Δ*redD*), Δ*dasR* (BAP29; Rigali *et al*., 2006) and GlcNAc uptake (BAP5 (Nothaft *et al*., 2010), Δ*nagE2*) null mutants were utilized in this work. Other streptomycetes used in this study are listed in Table S2. The iron-limited R2YE medium (3 μM final concentration) was used for siderophore production assays and phenotype studies. All media and routine *Streptomyces* techniques have been described previously (Kieser *et al*., 2000).

Siderophore production and extraction

Five hundred microlitres of *Streptomyces* spore suspensions (~ 10^8 spores ml^{-1}) were used to inoculate solid agar plates covered with cellophane disks (GE Osmonics Labstore, Ref K01CP09030). After growth at 28°C, mycelium was collected from the cellophane membrane and weighed for fresh biomass determination. Siderophores were extracted from the spent agar with an equal volume of MilliQ water, lyophilized, and finally resuspended in MilliQ water according to the measured biomass (fresh weight) for further comparative analyses.

Electrophoretic mobility gel shift assays (EMSA)

DasR-6His was produced in *Escherichia coli* BL21(DE3) and purified as previously described (Rigali *et al*., 2004; Colson *et al*., 2007). EMSA on double-stranded oligonucleotides were performed using 15 pmol of Cy5-labelled probes and different concentrations of DasR-6His (from 50 to 200 pmol) in a total reaction volume of 50 μl. All reactions were carried out in binding buffer (10 mM Tris-Cl pH 7.5, 1 mM DTT,

0.25 mM $CaCl_2$, 0.5 mM $MgCl_2$, 50 mM KCl and 2% glycerol) containing a 50-fold excess of non-specific DNA. After 20 min of incubation at room temperature, reaction mixtures were loaded into a 1% (w/v) agarose gel. Bound and unbound probes were separated by gel electrophoresis at room temperature and fluorescent DNA was visualized using a Typhoon Trio+ Variable Mode Imager (GE Healthcare) with a laser excitation at 633 nm and emission filter at 670 mM (BP30). The nucleotide sequences of oligonucleotides used to generate the *dre*^{dmdR1} probes were 5′-TGACACC GCACTGGTCCAGACCGCACCGTGATCC-3′ and 5′-CY5-GCATCACGGTGCGGTCTGGACCAGTGCGGTGTCA-3′.

Computational prediction of DasR-responsive elements in S. coelicolor

PREDetector (Hiard *et al*., 2007) was used to generate a weight matrix and predict positions of DasR-responsive elements (*dre*) in several streptomycetes. To generate the matrix we used 11 *dre* experimentally validated both *in vitro* and *in vivo* (Rigali *et al*., 2004; 2006; 2008; Colson *et al*., 2007; 2008; Swiatek *et al*., 2012). Sequences used to generate the weight matrix were those of *dre* upstream of *ptsH* (AGTTGTCTAGACCAGT), *malX2* (ACTGGTCTACACCAGT), *crr-ptsI* (TGTGGTCTAGACCTCT), *nagE2* (ACAGGTCTACACCACT), *nagB* (TGTGGTTTAGACCAAT), *nagA* (AGAGGTCTAGTCCACT), *ngcE* (AGTGGACTATACCTGT), *dasA* (ACTGGTCTACACCATT), SCO2946 (AGAGGTCTGAACCAAT), *redZ* (AGTGGTTTCCACCTCA) and *act*II-4 (TGTTGAGTAGGCCTGT). The cut-off score was set at 8.0 and *dre* were searched for within the first 300 nt upstream of annotated *S. coelicolor* genes (Bentley *et al*., 2002).

Semi-quantitative reverse transcription polymerase chain reaction (RT-PCR)

RT-PCR analyses were conducted with the QIAGEN One-Step RT-PCR Kit. RT-PCRs without reverse transcription were used as control for absence of residual DNA. For semi-quantitative analysis, samples were taken at three-cycle intervals between cycles 28 and 40 to compare non-saturated PCR product formation. Oligonucleotides used for *dmdR1, nagE2* and 16S rRNA amplification were 5′-ATGTACCTCCGCACCATCCTC-3′ and 5′-TCATCACGT GCTCCCAGCGAC-3′, 5′-GGCTGGGACAAGGTCGCCGCG GTC-3′ and 5′-CCCATGATGATGCCGCCGAGCACC-3′, and 5′-GTAACACAACAGCGAGGACG-3′ and 5′-TACCTCACC AACAAGCTGA-3′ respectively. Semi-quantitative measurement of the RT-PCR products was performed using Image J1.41o software.

High-performance liquid chromatography

Prior to injection, the siderophores of the extracts were converted to their ferric complexes by addition of $FeCl_3$. A Waters 2695 Separations Module HPLC with a Waters 996 Photodiode Array Detector was used for HPLC analysis. Samples were analysed on a nucleodur (Macherey-Nagel) C18ec column (250 × 4.6, 5 μm i.d., column temperature 20°C). Solvent A: MilliQ water + 0.1% trifluoroacetic acid (TFA); solvent B: acetonitrile 100% + 0.1% TFA. Elution started at A 100% and B increased gradually to 35% in 18 min. There followed a gradient bringing B to 100% in 1.5 min where it remained at 100% for 2 min. Following the isochratic conditions, A was brought to 100% in 2 min followed by a plateau at A 100% for 2 min. Ferric-tris-hydroxamate complexes were detected by monitoring A_{435} as reported previously (Barona-Gomez *et al*., 2006).

LC-ESI-MS analysis of siderophores

The siderophore extracts were analysed by reverse phase HPLC (HPLC Waters Alliance 2695/Diode Array Detector) coupled with a single quadrupole mass spectrometer (Waters SQD mass analyser) on an X-terra MS (Waters) 150 × 2.1 mm, 3.5 μm column. Siderophores were eluted by using an acetonitrile (ACN) gradient ranging from 0% to 35% in 20 minu (ACN and water were acidified with 0.1% formic acid) at 0.5 ml min^{-1} and 40°C. The identity of each siderophore was confirmed on the basis of the masses (molecular ions $[M+H]^+$) detected in the SQD by setting electrospray ionization source conditions in the MS as source temperature, 130°C; desolvation temperature, 250°C and nitrogen flow 500 l h^{-1}. The specific cone voltages used were 55 V for coelichelin and 80 V for desferrioxamines. The qualitative measurements of each siderophore were determined by comparing their corresponding peak area in the different extracts.

CAS assay for siderophore detection

Chrome azurol S medium was prepared according to Schwyn and Neilands (1987), without the addition of nutrients. The medium for 1 l of CAS was as follows: CAS 60.5 mg, hexadecyltrimetyl ammonium bromide (HDTMA) 72.9 mg, piperazine-1,4-bis(2-ethanesulfonic acid) (PIPES) 30.24 g and 1 mM $FeCl_3 \cdot 6H_2O$ in 10 mM HCl 10 ml. Agarose (0.9 w/v) was used as gelling agent. Wells were performed in the CAS media and filled with 150 μl of the extracts to achieve siderophore detection.

Acknowledgements

This work is supported by a FRIA fellowship from the FRS-FNRS to E.T., M.C., S.C. and S.L. and Grant R.CFRA. 1237 from the Fonds Spéciaux of the University of Liège for M.M. We are thankful to Laurent Franzil for his excellent technical assistance. S.R. is a research associate of the FRS-FNRS.

References

Andrews, S.C., Robinson, A.K., and Rodriguez-Quinones, F. (2003) Bacterial iron homeostasis. *FEMS Microbiol Rev* **27:** 215–237.

Barona-Gomez, F., Wong, U., Giannakopulos, A.E., Derrick, P.J., and Challis, G.L. (2004) Identification of a cluster of genes that directs desferrioxamine biosynthesis in

Streptomyces coelicolor M145. *J Am Chem Soc* **126:** 16282–16283.

Barona-Gomez, F., Lautru, S., Francou, F.X., Leblond, P., Pernodet, J.L., and Challis, G.L. (2006) Multiple biosynthetic and uptake systems mediate siderophore-dependent iron acquisition in *Streptomyces coelicolor* A3(2) and *Streptomyces ambofaciens* ATCC 23877. *Microbiology* **152:** 3355–3366.

Bentley, S.D., Chater, K.F., Cerdeno-Tarraga, A.M., Challis, G.L., Thomson, N.R., James, K.D., *et al*. (2002) Complete genome sequence of the model actinomycete *Streptomyces coelicolor* A3(2). *Nature* **417:** 141–147.

Bertram, R., Rigali, S., Wood, N., Lulko, A.T., Kuipers, O.P., and Titgemeyer, F. (2011) Regulon of the N-acetylglucosamine utilization regulator NagR in *Bacillus subtilis*. *J Bacteriol* **193:** 3525–3536.

Boelaert, J.R., de Locht, M., Van Cutsem, J., Kerrels, V., Cantinieaux, B., Verdonck, A., *et al*. (1993) Mucormycosis during deferoxamine therapy is a siderophore-mediated infection. *In vitro* and *in vivo* animal studies. *J Clin Invest* **91:** 1979–1986.

Boer, W., Folman, L.B., Summerbell, R.C., and Boddy, L. (2005) Living in a fungal world: impact of fungi on soil bacterial niche development. *FEMS Microbiol Rev* **29:** 795–811.

Braun, V. (1997) Avoidance of iron toxicity through regulation of bacterial iron transport. *Biol Chem* **378:** 779–786.

Colson, S., Stephan, J., Hertrich, T., Saito, A., van Wezel, G.P., Titgemeyer, F., and Rigali, S. (2007) Conserved cis-acting elements upstream of genes composing the chitinolytic system of streptomycetes are DasR-responsive elements. *J Mol Microbiol Biotechnol* **12:** 60–66.

Colson, S., van Wezel, G.P., Craig, M., Noens, E.E., Nothaft, H., Mommaas, A.M., *et al*. (2008) The chitobiose-binding protein, DasA, acts as a link between chitin utilization and morphogenesis in *Streptomyces coelicolor*. *Microbiology* **154:** 373–382.

Compant, S., Duffy, B., Nowak, J., Clement, C., and Barka, E.A. (2005) Use of plant growth-promoting bacteria for biocontrol of plant diseases: principles, mechanisms of action, and future prospects. *Appl Environ Microbiol* **71:** 4951–4959.

Cornelis, P., Wei, Q., Andrews, S.C., and Vinckx, T. (2011) Iron homeostasis and management of oxidative stress response in bacteria. *Metallomics* **3:** 540–549.

Crosa, J.H., and Walsh, C.T. (2002) Genetics and assembly line enzymology of siderophore biosynthesis in bacteria. *Microbiol Mol Biol Rev* **66:** 223–249.

Deutscher, J., Francke, C., and Postma, P.W. (2006) How phosphotransferase system-related protein phosphorylation regulates carbohydrate metabolism in bacteria. *Microbiol Mol Biol Rev* **70:** 939–1031.

Flores, F.J., and Martin, J.F. (2004) Iron-regulatory proteins DmdR1 and DmdR2 of *Streptomyces coelicolor* form two different DNA–protein complexes with iron boxes. *Biochem J* **380:** 497–503.

Floriano, B., and Bibb, M. (1996) *afsR* is a pleiotropic but conditionally required regulatory gene for antibiotic production in *Streptomyces coelicolor* A3(2). *Mol Microbiol* **21:** 385–396.

Galaris, D., and Pantopoulos, K. (2008) Oxidative stress and iron homeostasis: mechanistic and health aspects. *Crit Rev Clin Lab Sci* **45:** 1–23.

Greenwood, N.N., and Earnshaw, A. (1997) *Chemistry of the Elements*. Oxford, UK: Elsevier.

Hantke, K. (2001) Iron and metal regulation in bacteria. *Curr Opin Microbiol* **4:** 172–177.

Hiard, S., Maree, R., Colson, S., Hoskisson, P.A., Titgemeyer, F., van Wezel, G.P., *et al*. (2007) PREDetector: a new tool to identify regulatory elements in bacterial genomes. *Biochem Biophys Res Commun* **357:** 861–864.

Hoffmann, T., Schutz, A., Brosius, M., Volker, A., Volker, U., and Bremer, E. (2002) High-salinity-induced iron limitation in *Bacillus subtilis*. *J Bacteriol* **184:** 718–727.

Kieser, T., Bibb, M., Buttner, M.J., Chater, K.F., and Hopwood, D.A. (2000) *Practical Streptomyces Genetics*. Norwich, UK: John Innes Foundation.

Kincade, G.F., Saxton, G.D., Morse, P.W., and Mathisen, A.K. (1948) Streptomycin in the treatment of tuberculosis; a report of its use in a series of 100 cases. *Can Med Assoc J* **59:** 105–112.

Korgaonkar, A.K., and Whiteley, M. (2011) *Pseudomonas aeruginosa* enhances production of an antimicrobial in response to N-acetylglucosamine and peptidoglycan. *J Bacteriol* **193:** 909–917.

Lautru, S., Deeth, R.J., Bailey, L.M., and Challis, G.L. (2005) Discovery of a new peptide natural product by *Streptomyces coelicolor* genome mining. *Nat Chem Biol* **1:** 265–269.

Lee, J.W., and Helmann, J.D. (2007) Functional specialization within the Fur family of metalloregulators. *Biometals* **20:** 485–499.

Manteca, A., Fernandez, M., and Sanchez, J. (2005) A death round affecting a young compartmentalized mycelium precedes aerial mycelium dismantling in confluent surface cultures of *Streptomyces antibioticus*. *Microbiology* **151:** 3689–3697.

Manteca, A., Fernandez, M., and Sanchez, J. (2006) Cytological and biochemical evidence for an early cell dismantling event in surface cultures of *Streptomyces antibioticus*. *Res Microbiol* **157:** 143–152.

Matzanke, B.F., Bill, E., Trautwein, A.X., and Winkelmann, G. (1987) Role of siderophores in iron storage in spores of *Neurospora crassa* and *Aspergillus ochraceus*. *J Bacteriol* **169:** 5873–5876.

Miethke, M., and Marahiel, M.A. (2007) Siderophore-based iron acquisition and pathogen control. *Microbiol Mol Biol Rev* **71:** 413–451.

Miguelez, E.M., Hardisson, C., and Manzanal, M.B. (1999) Hyphal death during colony development in *Streptomyces antibioticus*: morphological evidence for the existence of a process of cell deletion in a multicellular prokaryote. *J Cell Biol* **145:** 515–525.

Nielsen, A.K., Breuner, A., Krzystanek, M., Andersen, J.T., Poulsen, T.A., Olsen, P.B., *et al*. (2010) Global transcriptional analysis of *Bacillus licheniformis* reveals an overlap between heat shock and iron limitation stimulon. *J Mol Microbiol Biotechnol* **18:** 162–173.

Nothaft, H., Dresel, D., Willimek, A., Mahr, K., Niederweis, M., and Titgemeyer, F. (2003a) The phosphotransferase system of *Streptomyces coelicolor* is biased for

N-acetylglucosamine metabolism. *J Bacteriol* **185:** 7019–7023.

Nothaft, H., Parche, S., Kamionka, A., and Titgemeyer, F. (2003b) *In vivo* analysis of HPr reveals a fructose-specific phosphotransferase system that confers high-affinity uptake in *Streptomyces coelicolor*. *J Bacteriol* **185:** 929–937.

Nothaft, H., Rigali, S., Boomsma, B., Swiatek, M., McDowall, K.J., van Wezel, G.P., and Titgemeyer, F. (2010) The permease gene *nagE2* is the key to N-acetylglucosamine sensing and utilization in *Streptomyces coelicolor* and is subject to multi-level control. *Mol Microbiol* **75:** 1133–1144.

Ratledge, C., and Dover, L.G. (2000) Iron metabolism in pathogenic bacteria. *Annu Rev Microbiol* **54:** 881–941.

Rigali, S., Schlicht, M., Hoskisson, P., Nothaft, H., Merzbacher, M., Joris, B., and Titgemeyer, F. (2004) Extending the classification of bacterial transcription factors beyond the helix–turn–helix motif as an alternative approach to discover new cis/trans relationships. *Nucleic Acids Res* **32:** 3418–3426.

Rigali, S., Nothaft, H., Noens, E.E., Schlicht, M., Colson, S., Muller, M., *et al*. (2006) The sugar phosphotransferase system of *Streptomyces coelicolor* is regulated by the GntR-family regulator DasR and links N-acetylglucosamine metabolism to the control of development. *Mol Microbiol* **61:** 1237–1251.

Rigali, S., Titgemeyer, F., Barends, S., Mulder, S., Thomae, A.W., Hopwood, D.A., and van Wezel, G.P. (2008) Feast or famine: the global regulator DasR links nutrient stress to antibiotic production by *Streptomyces*. *EMBO Rep* **9:** 670–675.

Schrempf, H. (2001) Recognition and degradation of chitin by streptomycetes. *Antonie Van Leeuwenhoek* **79:** 285–289.

Schwyn, B., and Neilands, J.B. (1987) Universal chemical assay for the detection and determination of siderophores. *Anal Biochem* **160:** 47–56.

Swiatek, M.A., Tenconi, E., Rigali, S., and van Wezel, G.P. (2012) Functional analysis of the N-acetylglucosamine metabolic genes of *Streptomyces coelicolor* and role in control of development and antibiotic production. *J Bacteriol* **194:** 1136–1144.

Touati, D. (2000) Iron and oxidative stress in bacteria. *Arch Biochem Biophys* **373:** 1–6.

Tunca, S., Barreiro, C., Sola-Landa, A., Coque, J.J., and Martin, J.F. (2007) Transcriptional regulation of the desferrioxamine gene cluster of *Streptomyces coelicolor* is mediated by binding of DmdR1 to an iron box in the promoter of the *desA* gene. *FEBS J* **274:** 1110–1122.

Wandersman, C., and Delepelaire, P. (2004) Bacterial iron sources: from siderophores to hemophores. *Annu Rev Microbiol* **58:** 611–647.

Yamanaka, K., Oikawa, H., Ogawa, H.O., Hosono, K., Shinmachi, F., Takano, H., *et al*. (2005) Desferrioxamine E produced by *Streptomyces griseus* stimulates growth and development of *Streptomyces tanashiensis*. *Microbiology* **151:** 2899–2905.

Young, G.M., and Postle, K. (1994) Repression of *tonB* transcription during anaerobic growth requires Fur binding at the promoter and a second factor binding upstream. *Mol Microbiol* **11:** 943–954.

Supporting information

Additional Supporting Information may be found in the online version of this article:

Fig. S1 (related to Fig. 1C). ESI-MS analysis of the three siderophores identified by HPLC in the crude extracts. The masses (molecular ions [M+H]+) of these three molecules correspond to (A) coelichelin (m/z = 566.45), (B) desferrioxamine B (m/z = 561.59) and (C) desferrioxamine E (m/z = 601.58) respectively.

Fig. S2 (related to Fig. 2B). Effect of *dasR* deletion and/or GlcNAc addition on siderophore production in *S. lividans*. CAS siderophore production assay of *S. lividans* TK24 and its *dasR* mutant. Extracellular extracts were obtained from mycelia grown for 72 h on R2YE plates with or without GlcNAc (50 mM). Note the less drastic reduction in siderophore production due to the inactivation of *dasR* than upon GlcNAc addition.

Table S1. List of DasR-responsive elements (*dre*) identified in *Streptomyces coelicolor*.

Table S2. List of *Streptomyces* strains used in this study.

Please note: Wiley-Blackwell are not responsible for the content or functionality of any supporting materials supplied by the authors. Any queries (other than missing material) should be directed to the corresponding author for the article.